

Electronic Supplementary Information

Superhydrophobic heterogeneous graphene networks with controllable adhesion behavior for detecting multiple underwater motions

Guomin Ding, Weicheng Jiao,* Rongguo wang, Meiling Yan, Zhenming Chu and Xiaodong He

Characterization. The optical micrograph of the emulsions was obtained using an RX50 M series metallurgical microscope (Sunny Optical Technology (group) CO. Ltd.). The morphology of the OCGN and PDMS/OCGNs was characterized using SEM on a Helios Nanolab 600i. The XPS spectra of samples were collected on a PHI 5700 ESCA System using an Mg K α line as the X-ray source. FTIR were recorded using a Tensor 27 from Bruker (using KBr pellets). The electrical conductivity was measured using a standard four-probe method with a Keithley 196 system DMM digital multimeter at room temperature. The viscosities of the PDMS-heptane solutions were measured using a rheometer, Bohlin Gemini HR Nano (Malvern Instruments) at room temperature with a shear rate of 15 s⁻¹. The WCA value was measured via a Dataphysics OCA20 contact-angle system. It is the average of five results at different positions on the same sample with a constant volume of water (4 μ L). The SA of water droplets was obtained via inclining the sample with an inclinable platform. The adhesive force of the different surfaces for water droplets was characterized using a high-sensitivity microelectromechanical balance (Dataphysics DCAT 21, Germany). A water droplet (5 μ L) was first suspended on a metal cap and fixed to the balance. Then, the stage with sample was placed below the water droplet and moved upwards at a constant speed of 0.02 mm s⁻¹. When the surface contacted the water droplet, the stage was moved down. The maximum force when the surface broke free from the water droplet was recorded as the adhesive force. The resistances of the samples were recorded using a UT71D intelligent digital multimeter (Uni-Trend Technology (China) Limited) connected to a computer.

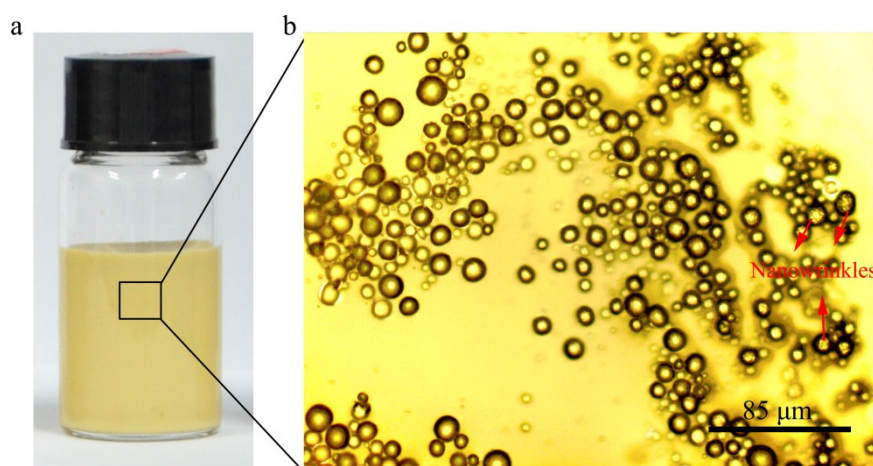


Fig. S1 (a) Photograph of frozen GO Pickering emulsion. (b) Micrograph of frozen GO Pickering emulsion with nanowrinkles.



Fig. S2 Photograph of PDMS/OCGN-10.

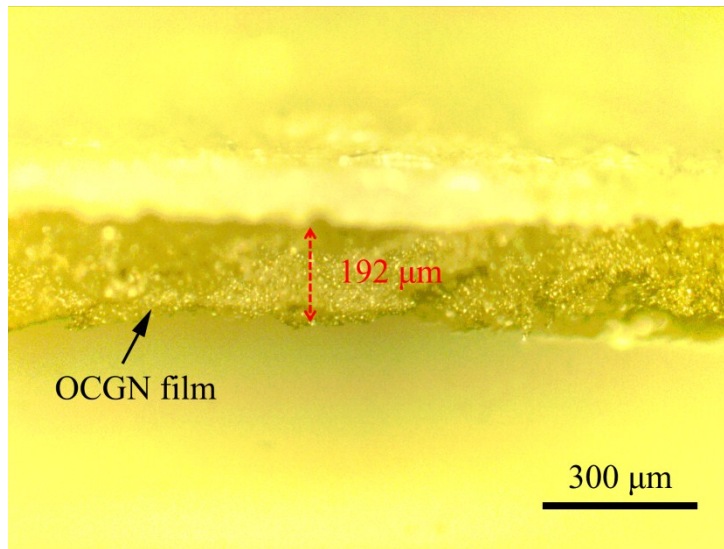


Fig. S3 Cross-sectional micrograph of OCGN film.

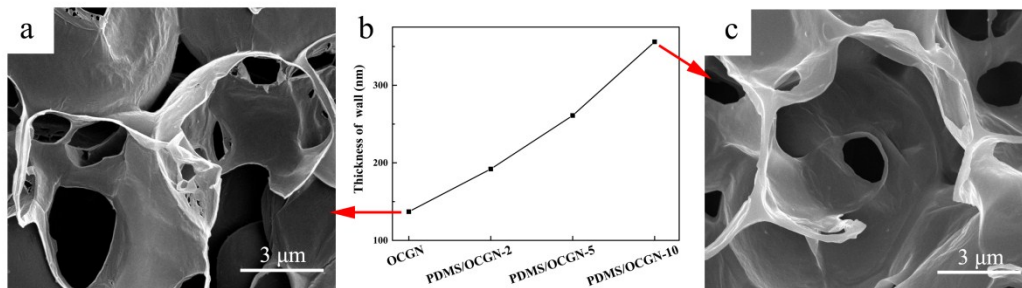


Fig. S4 (a) Magnified SEM image of the OCGN. (b) The change in wall thickness of the OCGN and PDMS/OCGNs. (c) Magnified SEM image of the PDMS/OCGN-10.

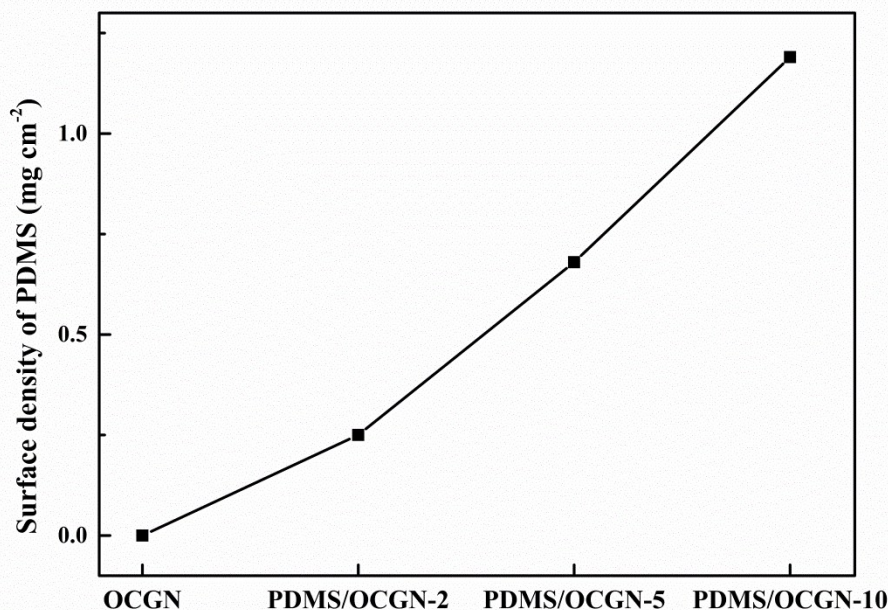


Fig. S5 The surface density of PDMS coating on different PDMS/OCGNs.

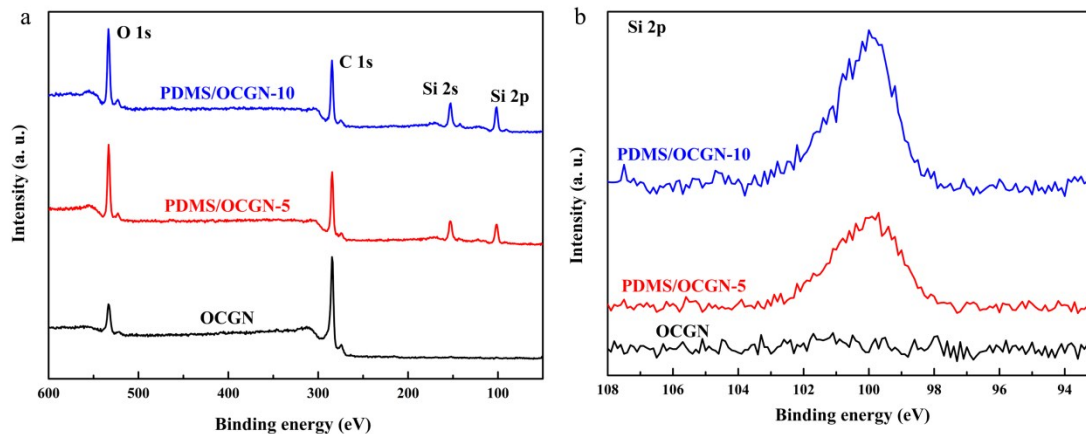


Fig. S6 (a) Survey scans of XPS spectra of the OCGN, PDMS/OCGN-5 and PDMS/OCGN-10. (b) Si 2p spectra of the OCGN, PDMS/OCGN-5 and PDMS/OCGN-10.

The chemical structures of the OCGN and PDMS/OCGNs surfaces were characterized by the XPS. As shown in the survey scan in Fig. S6a, the main elements on the OCGN surface are C and O, which is a typical feature for reduced graphene oxide.^{1,2} The atomic percentages of elements are also shown in the Table. S1. After PDMS functionalization, the peak of O 1s in PDMS/OCGN-5 spectrum becomes stronger obviously than that in the OCGN spectrum, which indicates that the content of O atoms increases (Table. S1). Meanwhile, two new peaks appear at 152 eV and 101 eV, which are attributed to Si 2s and Si 2p respectively (Fig. S6a).^{3,4} These changes are due to introduction of PDMS, which brings lots of O and Si atoms on surface. Moreover, the percentages of O and Si atom increase further on the surface of PDMS/OCGN-10, which verifies the increased content of PDMS coating (Table. S1). These changes are also proved by the Si 2p spectra of PDMS/OCGNs (Fig. S6b).

Table. S1 The atomic percentages of elements for different PDMS/OCGNs.

Element	Atomic percentage of OCGN (%)	Atomic percentage of PDMS/OCGN-5 (%)	Atomic percentage of PDMS/OCGN-10 (%)
C	89.8	57.9	49.7
O	10.2	21.7	24.6
Si	--	20.4	25.7

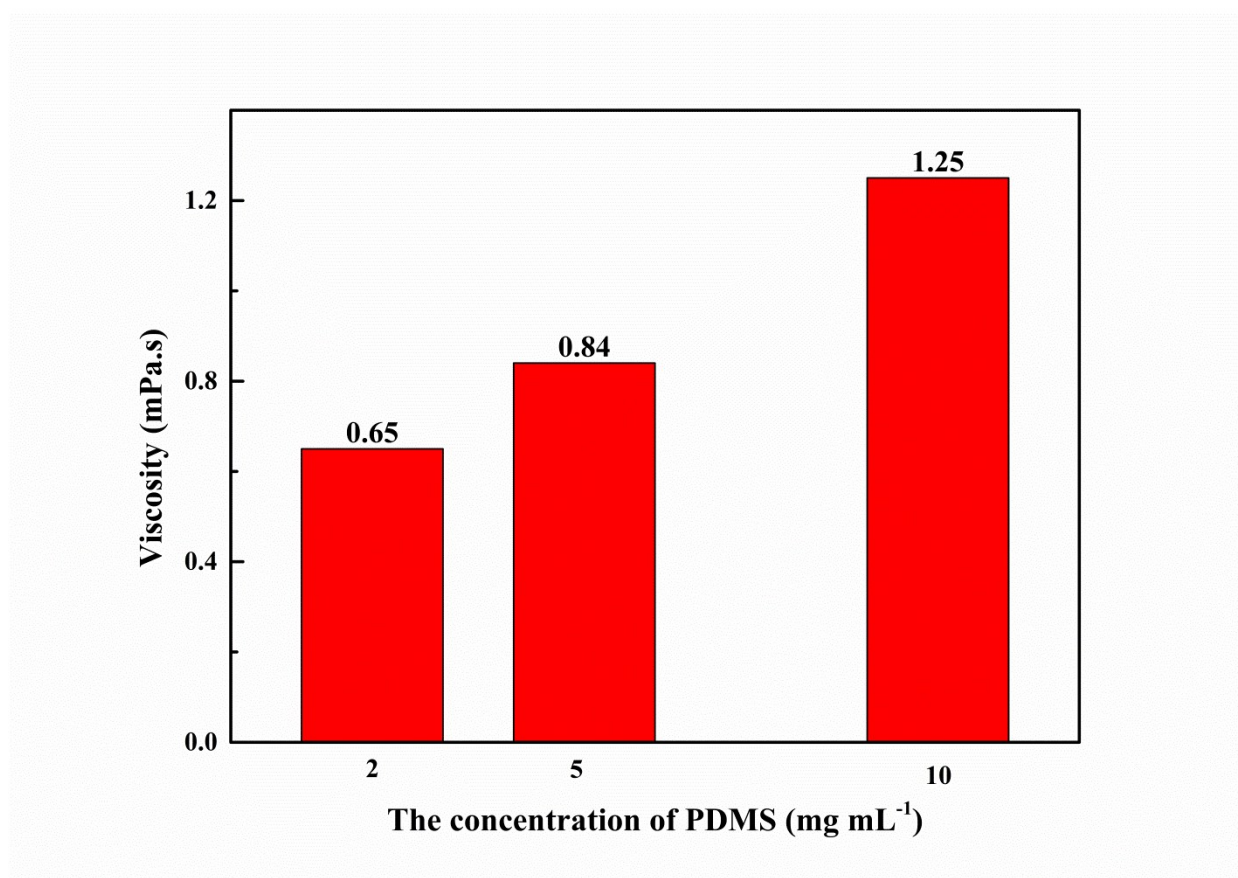


Fig. S7 The change of viscosity with the increase of concentration of PDMS.

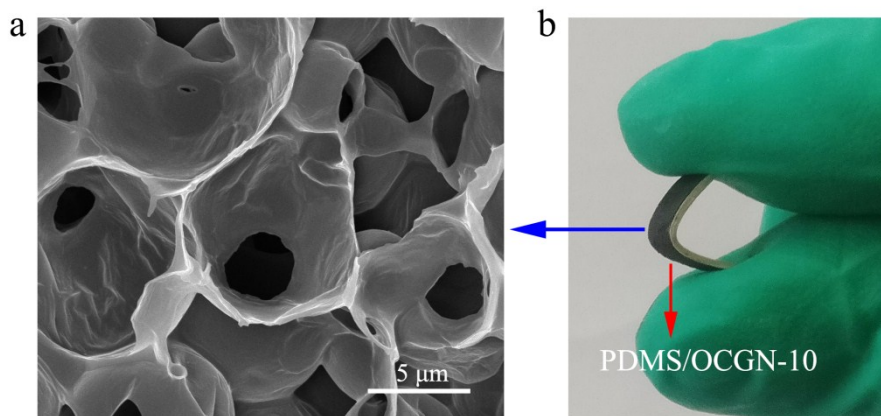


Fig. S8 a) The SEM image of PDMS/OCGN-10 after bent dozens of times. b) The bending experiment for the PDMS/OCGN-10.

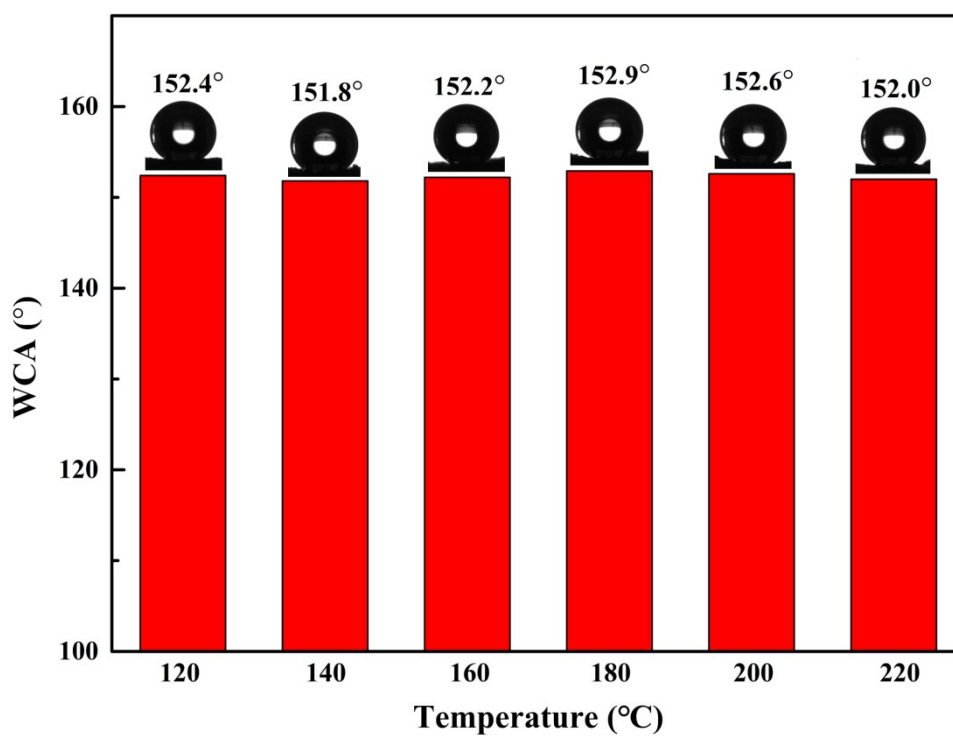


Fig. S9 The WCAs of PDMS/OCGN-10 after treated in different high temperature environment for 2 h. The insets are images of water droplet on corresponding surface.

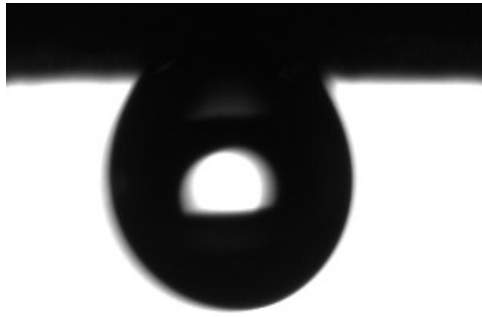


Fig. S10 A water droplet on OCGN when turned to 180°.

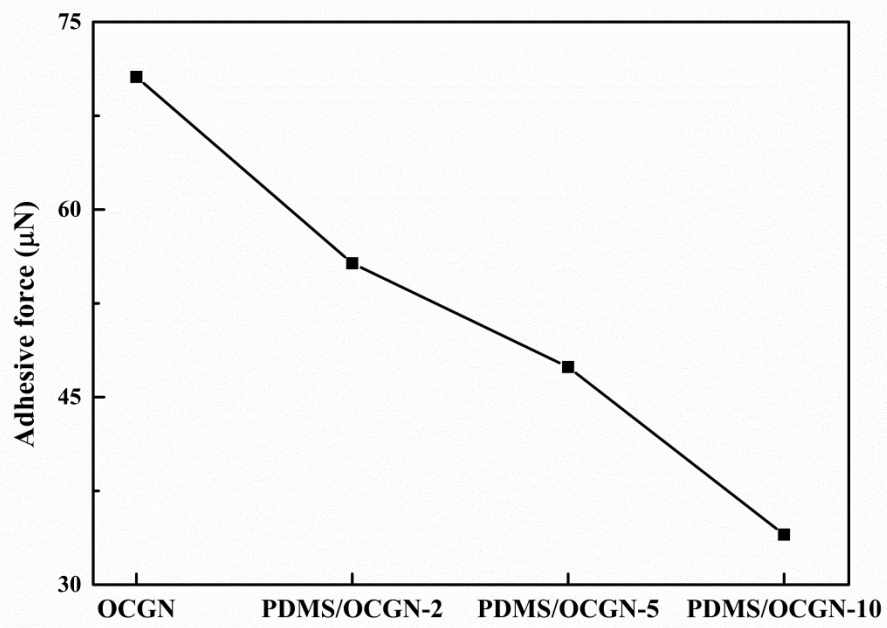


Fig. S11 The change in adhesive forces of different PDMS/OCGNs.

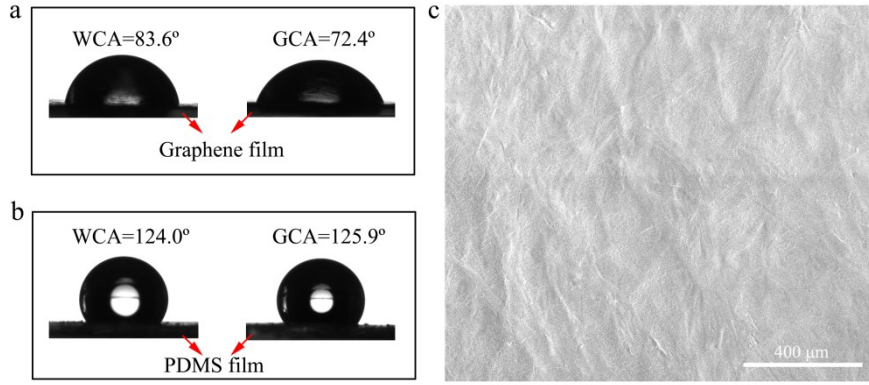


Fig. S12 (a) The images of water drop and glycerol drop on graphene surface. (b) The images of water drop and glycerol drop on PP coating surface. (c) The SEM image of graphene film.

The surface energies of graphene and PDMS were investigated by Owens–Wendt surface energy theory.^{5,6}

$$\gamma_l (\cos\theta + 1) / 2 = (\gamma_l^d)^{1/2}(\gamma_s^d)^{1/2} + (\gamma_l^p)^{1/2}(\gamma_s^p)^{1/2}$$

$$\gamma_s = \gamma_s^d + \gamma_s^p$$

where θ and γ_s were the contact angle and surface energy, and $\gamma_l^d, \gamma_l^p, \gamma_s^d$, and γ_s^p were the liquid dispersion component, liquid polar component, solid dispersive component, and solid polar component, respectively. So for calculating the surface energy, two kinds of liquid with known γ_l^d and γ_l^p would be necessary. Here, we used the water and glycerol. The dispersion and the polar components of water are 21.8 and 51.0 mJ m⁻², respectively, and those of glycerol are 37.0 and 26.4 mJ m⁻², respectively.³ Besides, It should be noted that in order to remove the influence of micro–nanoscale hierarchical structure, a graphene film with smooth surface was prepared by coated GO solution on glass slide and reduced in the HI vapor (Fig. S12c). Similarly, the PDMS film was obtained through cured on flat glass slide. The WCA and the glycerol contact angle (GCA) on corresponding surface are shown in Fig. S12. Finally, the surface energy values of graphene and PDMS were computed as 27.4 mJ m⁻² and 3.8 mJ m⁻², respectively. This indicates that PDMS has a lower surface energy than graphene.

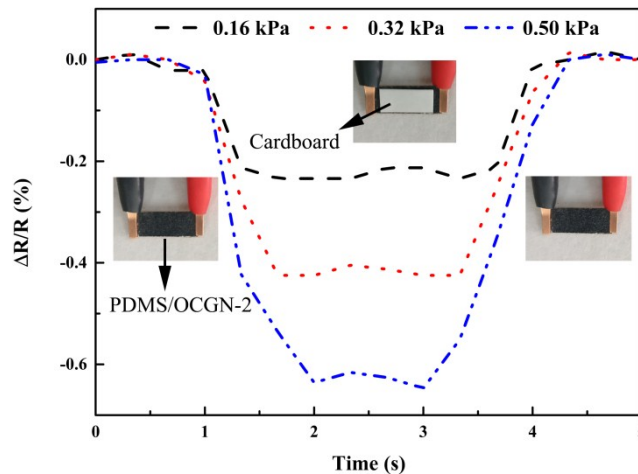


Fig. S13 Resistance change of PDMS/OCGN-2 with different pressures.

The effect of pressure on the resistance of PDMS/OCGN was explored by following method. The cardboards with varying weights were placed on the surface of PDMS/OCGN-2 to apply different pressures (inset in Fig. S13). The pressure (p) was calculated using $p=mg/s$, where m , s and g are the mass of the cardboards, area of the cardboards and acceleration of gravity (9.8 N kg⁻¹). As shown in Fig. S13, when cardboard was placed on the surface of PDMS/OCGN-2, the resistance

declined sharply, and after removed the weight, the resistance could recover. Moreover, as the pressure increased, the decrease of $\Delta R/R$ became great. This was due to that once the pressure was applied, the contact area between graphene nanosheets would become larger because of compressive deformation. Thus, the resistance of materials decreased. This change was similar to the resistance variation of PDMS/OCGN-2 during immersion and emersion processes, which verified indirectly the underwater sensing mechanism.

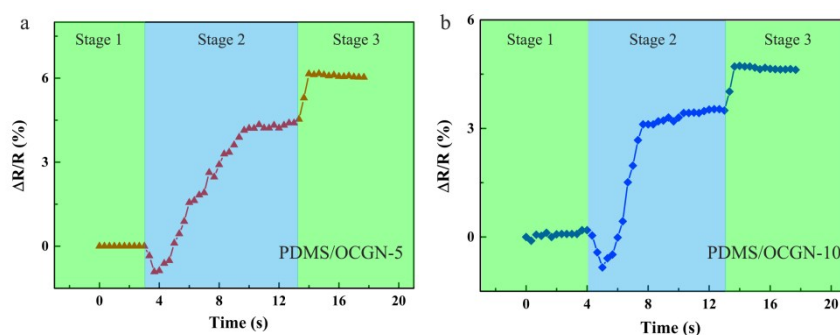


Fig. S14 (a) The change of $\Delta R/R$ of PDMS/OCGN-5 during immersion and emersion processes. (b) The change of $\Delta R/R$ of PDMS/OCGN-10 during immersion and emersion processes.

Notes and references

- 1 S. Pei, J. Zhao, J. Du, W. Ren and H.-M. Cheng, *Carbon*, 2010, **48**, 4466-4474.
- 2 H. Huang, Y. Tang, L. Xu, S. Tang and Y. Du, *ACS Appl. Mater. Interfaces*, 2014, **6**, 10248-10257.
- 3 X. Chen, J. A. Weibel and S. V. Garimella, *Ind. Eng. Chem. Res.*, 2016, **55**, 3596-3602.
- 4 X. Su, H. Li, X. Lai, L. Zhang, J. Wang, X. Liao and X. Zeng, *ACS Appl. Mater. Interfaces*, 2017, **9**, 28089-28099.
- 5 D. K. Owens and R. C. Wendt, *J. Appl. Polym. Sci.*, 1969, **13**, 1741-1747.
- 6 Z. Bo, Y. Tian, Z. J. Han, S. Wu, S. Zhang, J. Yan, K. Cen and K. Ostrikov, *Nanoscale Horiz.*, 2017, **2**, 89-98.
- 7 D. Khang, S. Y. Kim, P. Liu-Snyder, G. T. R. Palmore, S. M. Durbin and T. J. Webster, *Biomaterials*, 2007, **28**, 4756-4768.